Electronic supplementary materials
For https://doi.org/10.1631/jzus.A2500282

Simulation and experimental analysis of grease injection process in the main drive seal lubrication structure of tunnel boring machines

Zheming TONG[1,2], Yuchen ZHAO[1,2], Lianhui JIA[3], Xiaolei Zhou[3], Haoxiang Lu[1,2], Wenqi NIU[3]

[1]*State Key Laboratory of Fluid Power and Mechatronic Systems, Zhejiang University, Hangzhou 310058, China*
[2]*School of Mechanical Engineering, Zhejiang University, Hangzhou 310058, China*
[3]*China Railway Engineering Equipment Group Co Ltd, Zhengzhou 450016, China*

Research Significance

During TBM tunneling, the underground environment is highly complex. The manufacturing accuracy, assembly precision, and operating conditions of the components directly affect the sealing performance. This performance, in turn, influences the service life of the main bearing. Nevertheless, numerical investigations under dynamic operating conditions remain scarce. In this study, a numerical simulation of the grease injection process within the main drive sealing system is conducted. The grease flow rates and pressure distributions in the cavity are examined under varying eccentricities, numbers of injection ports and inner wall rotation speeds. The results are used to optimize the sealing structure, improve its ability to prevent external contaminant intrusion, and extend the service life of the main drive system.

Section S1 Material properties

EP2 grease maintains good lubrication and thermal stability under heavy load conditions. When mixed with HBW sealing grease, EP2 enhances the overall sealing effect of the grease. This type of grease is widely used in large tunnel boring machines and other heavy-duty excavation equipment.

A rheological test was conducted on EP2 grease to obtain the relationship between grease viscosity and shear strain rate. The fitted results revealed that this relationship can be described by an exponential function. Therefore, a power-law constitutive

equation is adopted in this study to represent the rheological properties of the grease. This model is suitable for describing non-Newtonian fluids exhibiting pseudoplasticity and dilatancy. Under this model, the shear stress τ of the non-Newtonian fluid can be characterized by an exponential function, as expressed in Eq. (S1), where ϕ is the consistency index, $\dot{\gamma}$ is the shear strain rate, and n is the flow behavior index.

$$\tau = \phi \cdot \dot{\gamma}^{n} \tag{S1}$$

When the flow behavior index equals 1, the corresponding constitutive equation describes a Newtonian fluid. When $n < 1$, the fluid exhibits pseudoplastic behavior, meaning its viscosity decreases with increasing shear rate. Conversely, when $n > 1$, the fluid demonstrates dilatant behavior, characterized by an increase in viscosity with increasing shear rate.

Section S2 Experiment procedure

The main drive sealing test platform is designed to investigate the conditions of grease diffusion, lubrication sealing, and other states under both atmospheric and negative pressure. The total weight of the test platform is approximately 15 tons, with a total power of about 60 kW. The rotational speed is adjustable from 0 to 40 r/min, allowing real-time observation of grease overflow conditions. The seals can be installed in both forward and reverse orientations, freely combined, and synchronized for experimentation. A fractional factorial design is employed, and each parameter setting is replicated twice to obtain the EP2 grease distributions.

The main drive labyrinth seal chamber is equipped with eight oil inlet ports as the original working condition around one revolution, filled with EP2 grease. At one end of the test platform, a motor is installed to drive the sealing ring at various speeds, simulating actual working conditions. The experimental platform has two labyrinthine cavity regions at the left and right ends, each formed by the interaction of end caps and outer cylinder labyrinth structures. On the right side, the labyrinth structure forming the right labyrinthine cavity retains a portion of empty volume. In subsequent

experiments, the structure of the labyrinthine cavity can be altered by replacing the right end cap, allowing for an investigation into the impact of labyrinth length on grease distribution. In this study, we filled the empty volume on the right side without considering its influence on grease distribution.

Additionally, within the chamber, four lip seals are installed, comprising two reverse lip seals on the left and two forward lip seals on the right. These lip seals are assembled and fixed with different-spaced rings. Around the periphery of the experimental platform, uniformly distributed oil injection ports with the same diameter are present. Upon oil injection initiation, grease is simultaneously injected through these ports into the fluid domain under the influence of external high pressure. The end caps on both sides of the labyrinthine cavity are fitted onto the ends of the inner cylinder with an interference fit. When the motor is started, the end caps rotate along with the inner cylinder to simulate the sealed lubrication of the actual main drive structure inside.

Section S3 Experiment results

It can be observed that the amount of grease leakage increases gradually with increasing eccentricity. In addition, a higher inner wall rotational speed causes the grease to accumulate at the lower part of the cavity, accompanied by a significant increase in leakage. Therefore, reducing the eccentricity and inner wall rotational speed within a certain range can effectively enhance the sealing performance of the main drive sealing system.

It can be observed that when the eccentricity is 0.75 mm, the diffusion arc length of the grease at the seal outlet accounts for approximately one-half of the total outlet arc length. When the eccentricity increases to 1.5 mm, the diffusion arc length is slightly less than two-thirds of the total arc length, but still significantly larger than one-half. At an eccentricity of 2.5 mm, the diffusion arc length exceeds two-thirds of the total arc length. Moreover, as the rotational speed increases, the diffusion arc length of EP2 grease also increases markedly, further confirming that greater eccentricity and higher inner wall rotational speed reduce the sealing effectiveness of the main drive sealing

system.

Section S4 Simulation model establishment

In this paper, concentricity, static roundness, and dynamic rotational speed are focused on, combined with experimental tests, to identify optimization directions of EP2 oil injection methods. During the grease injection process, when the oil pressure increases to a certain level, the lip seals undergo deformation under the influence of the oil pressure. This deformation allows the previously sealed adjacent chambers to become connected. This phenomenon is referred to as the fluid-structure interaction between the grease and the lip seals. As this study primarily focuses on the simulation of grease injection at the scale of the entire flow channel, the coupling effect between the grease and the lip seals is temporarily excluded from the simulation. To ensure that the chambers formed between adjacent lip seals can be interconnected for subsequent simulations, a fixed opening gap is defined between the lip seals and the inner and outer cylinders in the model. This design allows the chambers formed by neighboring lip seals to communicate with each other, facilitating the continuity of the simulation.

Section S5 Grease injection process under the original operating condition

From the start of injection to t = 1400 s, due to the significant difference between the grease flow velocity and the tangential velocity of the rotating inner cylinder, most of the grease is influenced by gravity and the agitation of the rotating inner wall, accumulating at the lower part of the fluid domain. Only a small amount of grease adheres to the surface of the inner cylinder in the middle region of the flow field, with a volume fraction of about 10%. By t = 2800 s, while grease continues to accumulate at the lower part of the flow field, the agitation from the rotating inner wall causes more grease to form a ring on the side of the stationary wall. At this point, the grease accounts for roughly one-fourth of the total flow field volume. At t = 4200 s, the grease begins to diffuse along the X-axis toward both sides, filling nearly half of the fluid domain volume. By t = 5400 s, the motor side of the sealing chamber becomes

more filled with grease, and the grease diffusing toward the non-motor side also begins to adhere to the rotating wall surface.

After 7000 seconds of injection, the motor side of the sealing chamber is nearly filled with grease. However, due to the larger radial width of the flow channel on the non-motor side, an unfilled cavity volume remains on that side. To verify whether the grease has stably filled the chamber, the injection was continued until 9000s. A comparison of the grease volume fraction contour plots at 7000s and 9000s shows that there is no significant change in the grease distribution within the chamber, and the unfilled region on the non-motor side of the seal remains. The flow stability of EP2 grease inside the chamber is assessed by analyzing the volume changes of the grease. As the grease begins to overflow from both side outlets within the fluid domain, the volume fraction starts to slightly decrease from 5700s onward, then fluctuates steadily within the range of 0.52 to 0.53.

Supplementary Tables

Table S1 Physical property parameters of EP2 grease

Grease	Power-law index n	ϕ / $(kg \cdot s^{(n-2)} \cdot m^{-1})$	Density/ $kg \cdot m^{-3}$
EP2	0.19609	305.25783	1100

Table S2 Indoor experiment working condition

Concentricity error/mm	Injection ports per chamber	Replication time	Inner wall rotational speed
0.75,1.5,2.5	8	2	5rpm,10rpm

Table S3 The grid structure of the original flow field

Mesh location	Mesh shape
The motor side	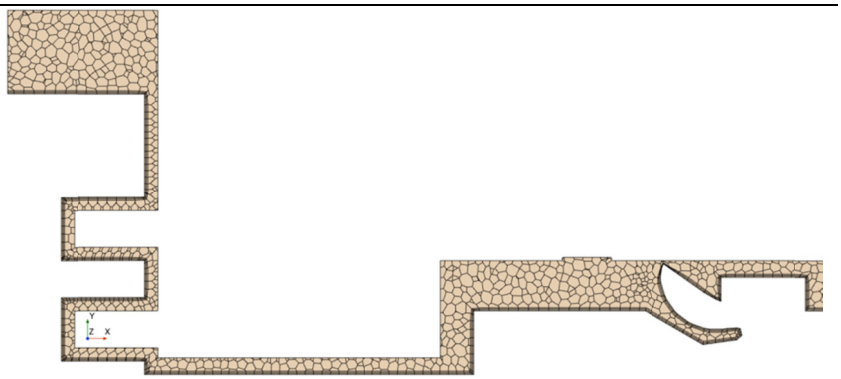
Non-motor side	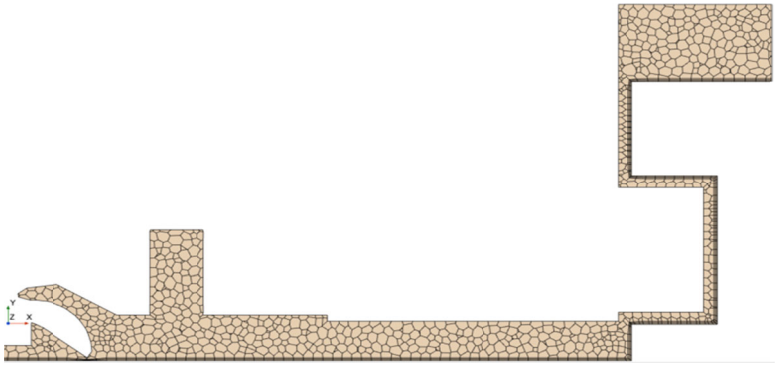

Table S4 EP2 grease distribution of each chamber under different eccentricities.

Eccentricity	EP2 grease distribution in the YOZ cross-section of each chamber				
	Motor side			Non-motor side	
	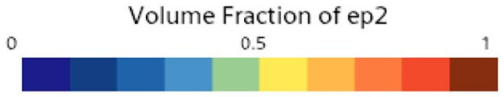				
	P0	P1	P2	P1	P0
0	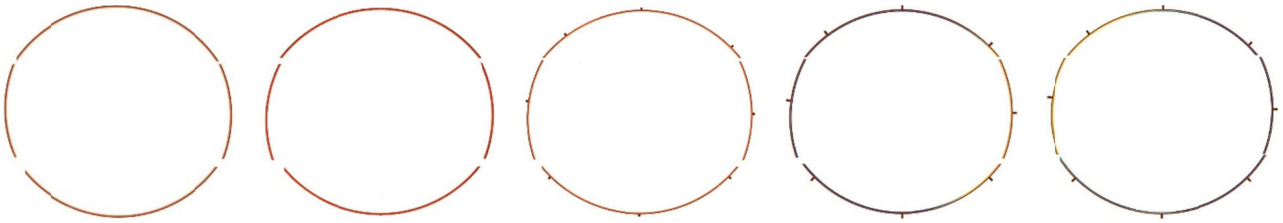				
0.75	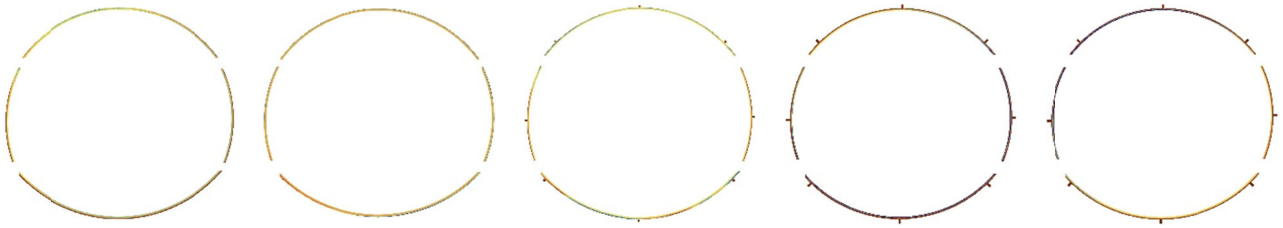				
1.5					
2.5					
3.5					

Table S5 EP2 grease distribution of each chamber with different numbers of injection ports

Number	EP2 grease distribution in the YOZ cross-section of each chamber				
	Motor side			Non-motor side	
	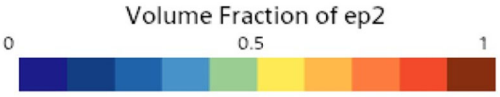				
	P0	P1	P2	P1	P0
20					
60	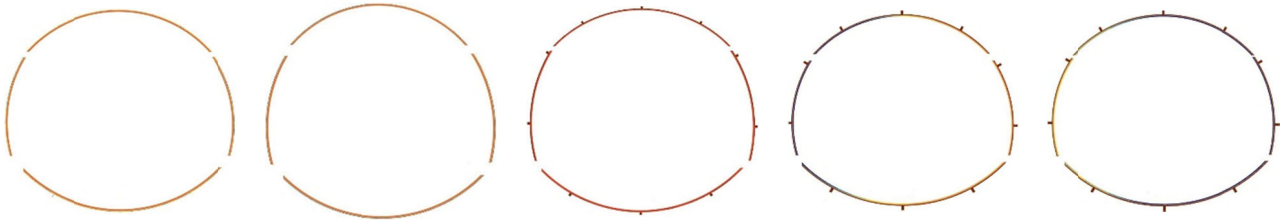				

Table S6 EP2 grease distribution of each chamber with different inner wall rotation speeds

Speed	EP2 grease distribution in the YOZ cross-section of each chamber				
	Motor side			Non-motor side	
	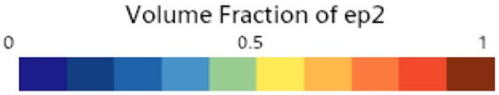				
	P0	P1	P2	P1	P0
5rpm	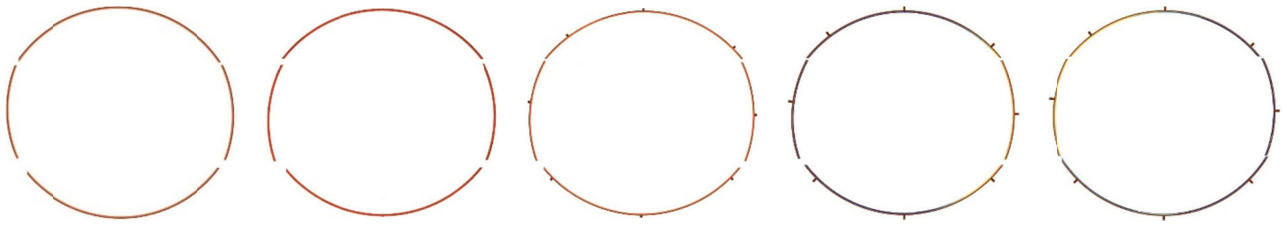				
10rpm	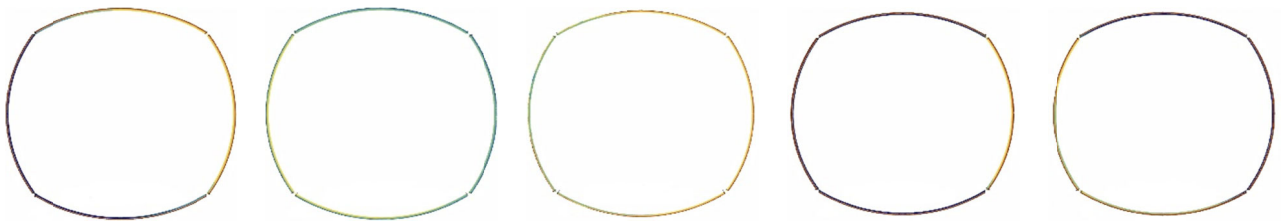				

Supplementary Figures

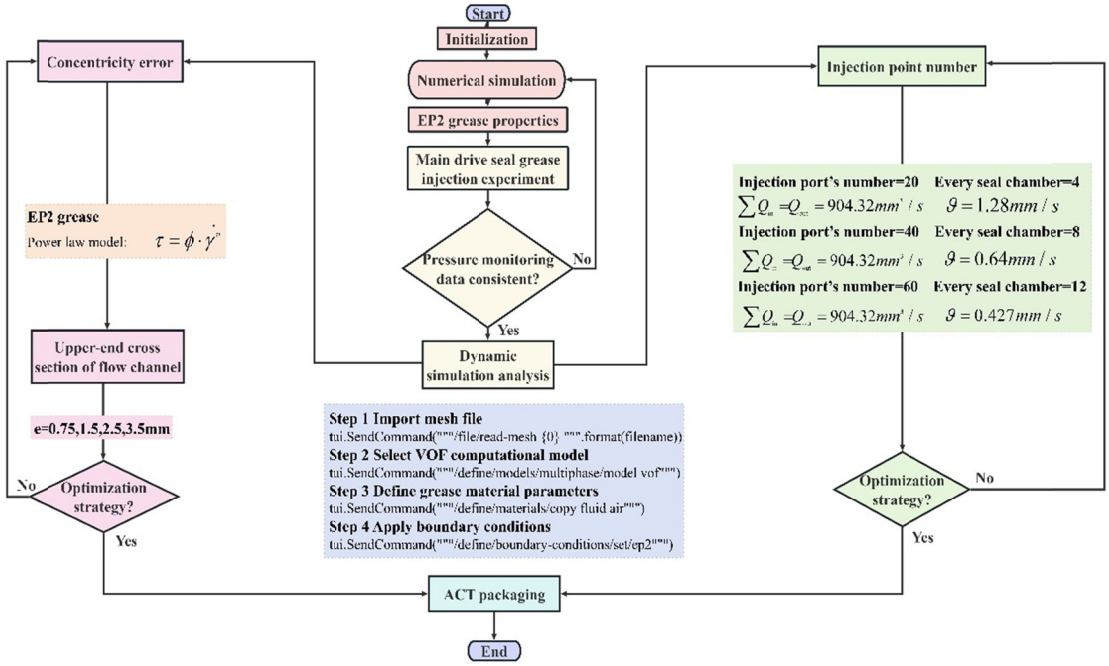

Fig. S1 Flow chart of study on the dynamic characteristics of grease injection in main drive seal

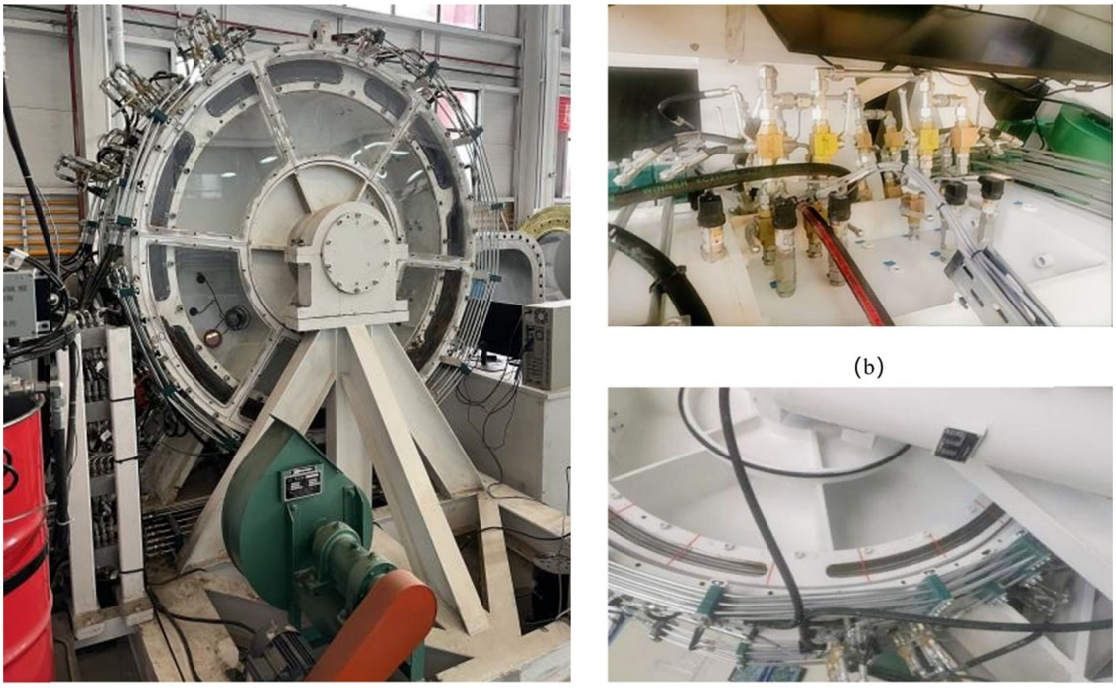

Fig. S2 Experiment test platform. (a) sealing system on the non-motor side (b) EP2 grease injection ports (c) Transparent end cap on motor side

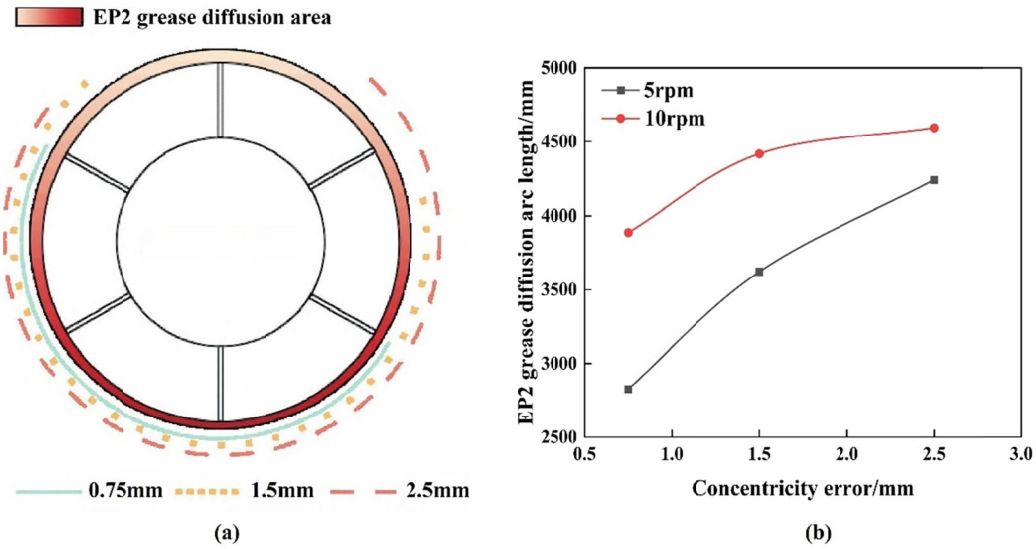

Fig. S3 EP2 grease diffusion results (a**)** diffusion area with different concentricity errors (b) diffusion arc length with different inner wall rotation speeds

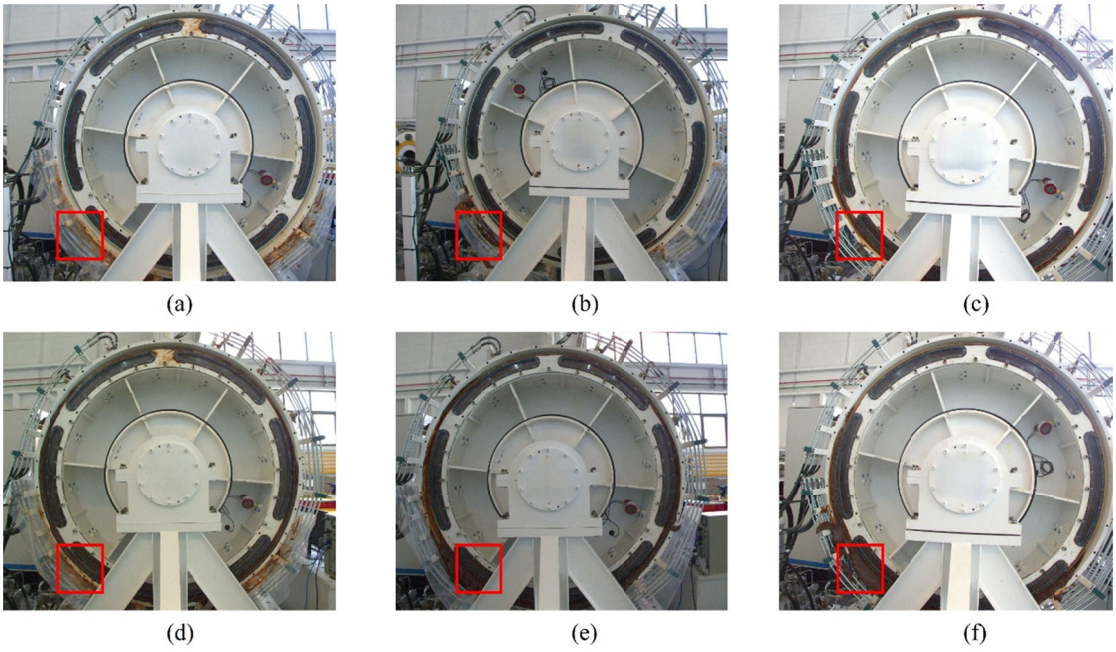

Fig. S4 EP2 overflow situation on non-motor side after two hours (a) concentricity error=0.75mm, inner wall rotational speed=5rpm (b) concentricity error=1.5mm, inner wall rotational speed=5rpm (c) concentricity error=2.5mm, inner wall rotational speed=5rpm (d) concentricity error=0.75mm, inner wall rotational speed=10rpm (e) concentricity error=1.5mm, inner wall rotational speed=10rpm (f) concentricity error=2.5mm, inner wall rotational speed=10rpm

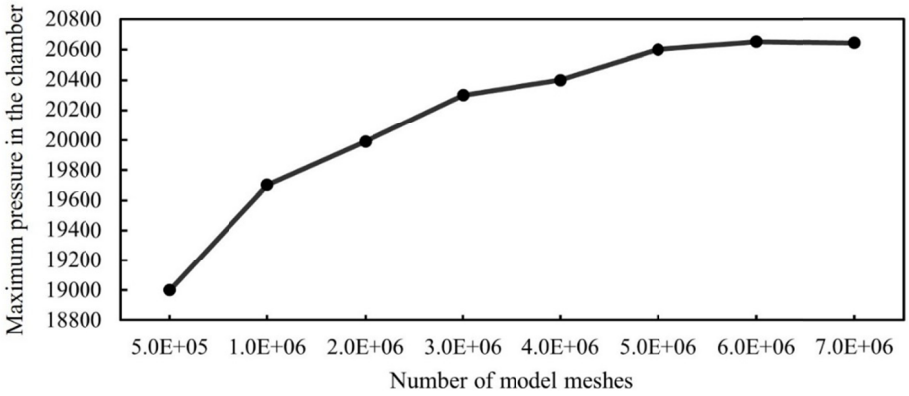

Fig. S5 Mesh independence verification

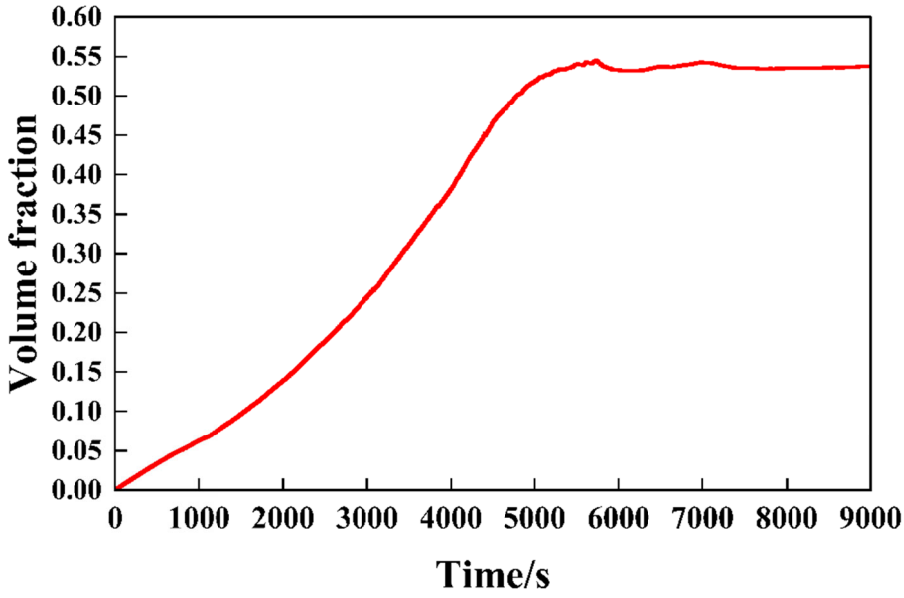

Fig. S6 The volume fraction of EP2 inside the chamber during the injection process

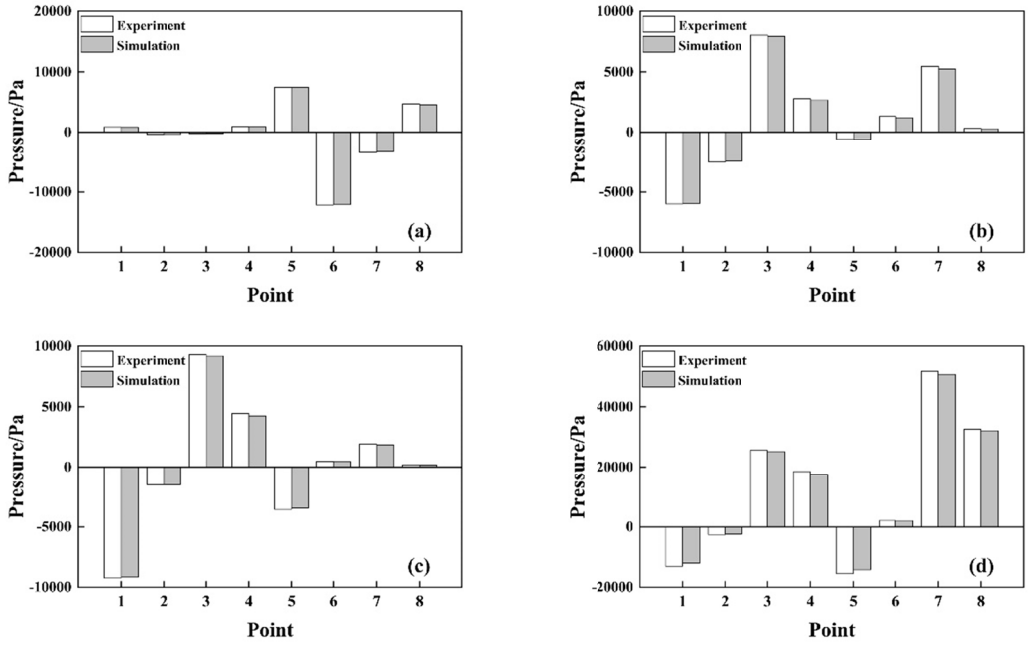

Fig. S7 Pressure comparison at monitoring points under different eccentricities of fluid domain (a) original condition (b) e=0.75mm (c) e=1.5mm (d) e=2.5mm